

Original article

# Organic Geochemistry of the Hot Shale Member of the Tanezzuft Formation of wells B1-23 and Q1-23, Ghadames Basin, NW Libya with Regional Correlation

Abdulhamid Boshnyf<sup>1</sup>, Osama Shaltami<sup>2\*</sup>, Anis Belhaj<sup>1</sup>, Mustafa Ben Hkoma<sup>3</sup>

<sup>1</sup>Sirte Oil Company, Libya

<sup>2</sup>Department of Earth Sciences, Faculty of Science, University of Benghazi, Libya

<sup>3</sup>Libyan Centre for Studies and Researches of Sciences and Environment Technology, Middle Zone Branch, Zliten, Libya

\*Correspondence. [osama.rahil@yahoo.com](mailto:osama.rahil@yahoo.com)

## Abstract

The present work is a source rock assessment of the Hot Shale Member of the Tanezzuft Formation (Early Silurian) using data obtained from wells B1-23 and Q1-23, Ghadames Basin, NW Libya. The geochemical data obtained from HAWK instrument analysis done by Sirte Oil Company on a number of shale samples representing the Hot Shale Member. In terms of organic richness, the Hot Shale Member falls between good and excellent based on the TOC values (1.05-12.39%). The binary plot of TOC versus PP backs up this assumption. In terms of kerogen type, the HI values (126-794 mg/g) display the ex-istence of different types of kerogens, such as types I, II, and III. The binary plots of Tmax versus HI, TOC versus S2, and OI versus HI offer more proof for this hypothesis. In terms of indigeneity, the dominance of indigenous hydrocarbons is suggested by the S1/TOC ratio (0.16-0.81). The binary plot of TOC versus S1 lends credence to this assumption. In terms of thermal maturity, the values of Tmax (417-441 oC) and Ro (0.3-0.78%), and the binary plots of Tmax versus HI, Tmax versus Ro, and PI versus Tmax indicate that the samples of well Q1-23 are primarily contain mature organic matter, whereas the majority of the samples of well B1-23 contain immature organic matter. In terms of petroleum potential, the Hot Shale Member exhibits a variety of petroleum potential, as shown by the binary plot of TOC versus HI. In terms of kinetic parameters, the activation energies (47-84 kcal/mol) have a gaussian shape.

**Keywords.** Organic Geochemistry, Source Rock, Hot Shale Member, Tanezzuft Formation, Ghadames Basin, Libya.

## Introduction

Desio [1] provided the first definition of the Tanezzuft Formation. The Wadi Tanezzuft in the Murzuq Basin is the type locality; however, Desio [1] did not identify the base and top of the formation at the type locality. Klitzsch [2] described the complete section of the formation at south Ghat. In this site the total thickness is 370 m and the formation is mainly composed of graptolitic shales with lesser amounts of siltstone and sandstone. There is an unconformable contact with the underlying Mamuniyat Formation, while there is a gradual transition with the overlying Akakus Formation [1]. There are two members of the Tanezzuft Formation; the Hot Shale Member at the base and the Cold Shale Member on top. The Hot Shale Member is composed of black shale that has high TOC content. The member is distinguished by unusually high radioactivity levels that are strongly linked to uranium existence [3]. Based on the palynostratigraphic and palynofacies, El Diasty [4] proposed ages of Early-Middle Rhuddanian (Early Silurian) and Late Rhuddanian-Telychnian (Early Silurian) for the Hot Shale Member and the Cold Shale Member, respectively. The sedimentological characteristics suggested that the Hot Shale Member was deposited in restricted to open marine environments [5].

The Ghadames Basin is considered one of the main sedimentary basins in Libya. It is a sizable intracratonic sag basin. It has an area of 350,000 km<sup>2</sup>. The depocentre of the basin is situated in Algeria. The eastern side of the basin is represented by the Libyan part, which rises to the Tripoli-Tibesti Arch and including the Zamzam Depression which stretches towards the east [6]. Up to 21,000 ft of basin-fill can be found in Algeria, but no more than 18,000 ft can be found in Libya. Its boundaries are the Dahar-Nafusah Arch to the north, the Hoggar Massif in Algeria and the Qarqaf Arch in Libya to the south, and the Amguid-El Biod Uplift in Algeria to the west. The basin protrudes beneath the western portion of the Sirte Basin to the east. Fig. 1 shows the time stratigraphic chart of west Libya.

The Ghadames Basin contains large reserves of gas (2.4 Tcf) and oil (64 MM bbl of oil and 39 MM bbl of condensates) in Libya. The majority of the Libyan discoveries are found in the Silurian and Devonian reservoirs, with minor discoveries in the Triassic deposits [6]. There are two proved source rocks in the Ghadames Basin: (1) The Hot Shale Member of the Tanezzuft Formation (Early Silurian); and (2) The Awaynat Wanin/Frasnian Shale (Late Devonian).

In this work, a geochemical evaluation of the Hot Shale Member of the Tanezzuft Formation was conducted in wells B1-23 and Q1-23, Ghadames Basin, NW Libya (Fig. 2). This evaluation included the following: (1) Organic richness; (2) Kerogen type; (3) Indigeneity; (4) Thermal maturity; (5) Petroleum Potential; and (6)

Kinetic Parameters. Fig. 3 shows regional correlation of gamma-ray profiles through the Hot Shale Member between the studied wells and wells J1-23, A1-61, and E1-23.

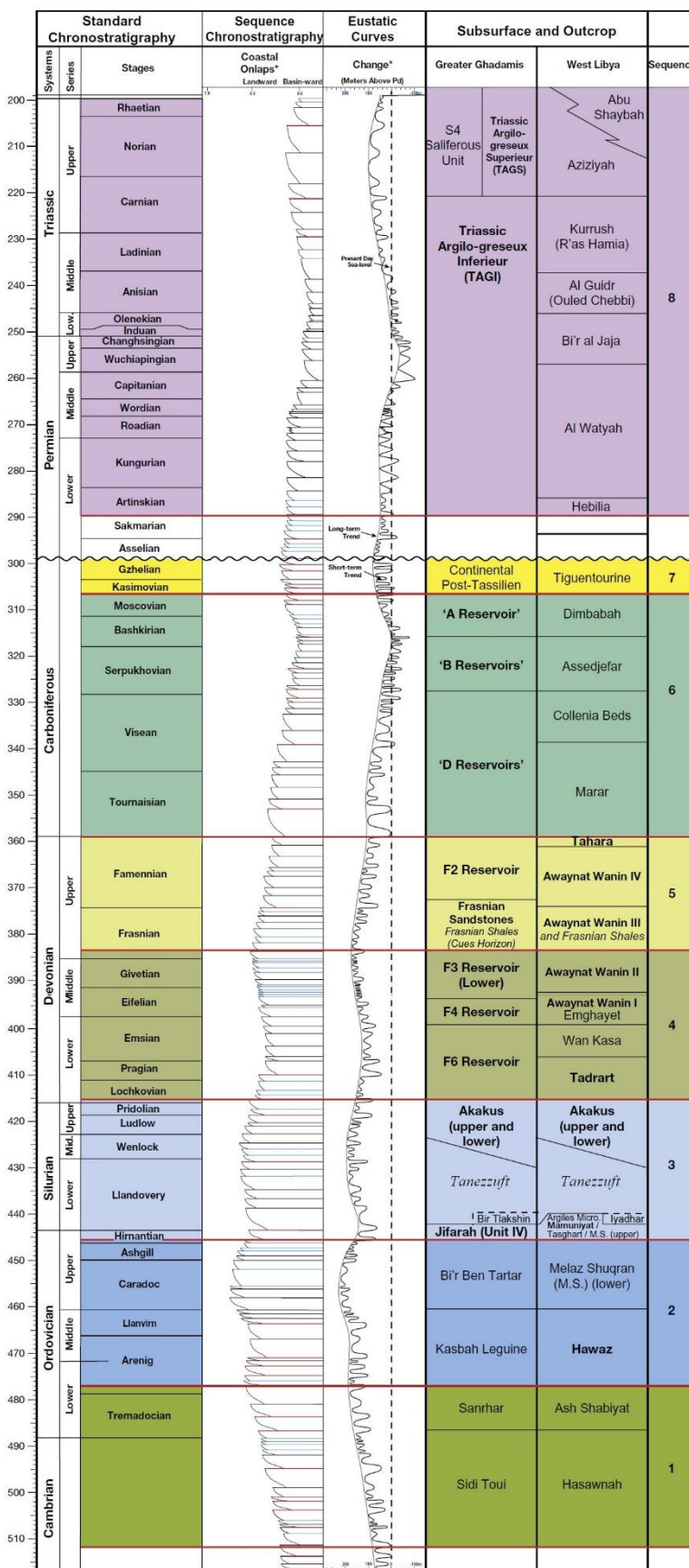


**Figure 1. Time stratigraphic chart of west Libya (bold lettering indicates petroleum reservoir; italic script indicates source rock) (after [19-21]).**

## Previous Work

With the exception of wells B1-23 and Q1-23, there have been numerous prior geochemical studies of the Hot Shale Member in many wells in the Ghadames and Murzuq basins [7-18].

## Methods

In this study, geochemical data provided by Sirte Oil Company were used. The following steps were followed in order to complete the current work:

(1) Seventeen cutting shale samples were selected from wells B1-23 (at depths 4595.28 to 4733ft) and Q1-23 (at depths 9652 to 9773.62ft).

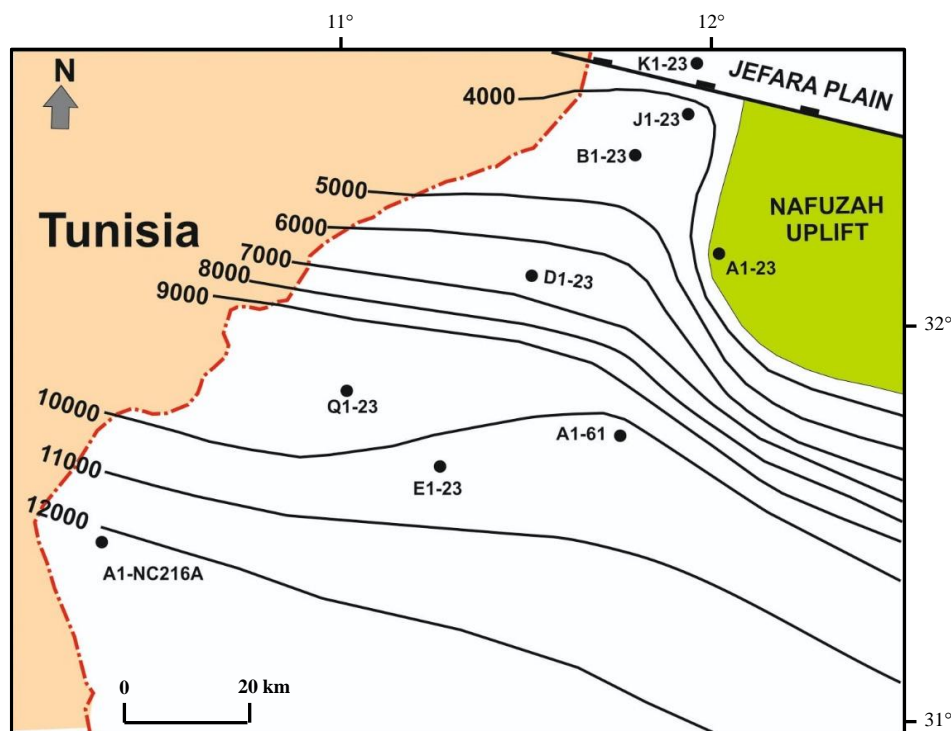


**Figure 2. Location map of wells B1-23, Q1-23, J1-23, A1-61, and E1-23.**

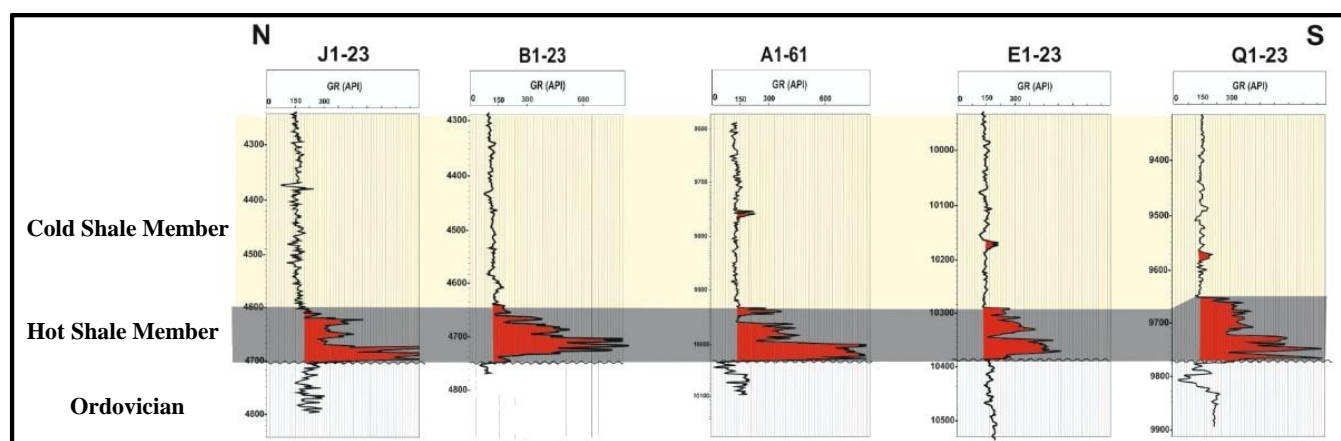


**Figure 3. Regional correlation of gamma-ray profiles through the Hot Shale Member in five wells in the Ghadames Basin.**

(2) The HAWK Pyrolysis was used to determine the values of TOC, S<sub>1</sub>, S<sub>2</sub>, S<sub>3</sub>, T<sub>max</sub>, Ro, HI, OI, PI, CaCO<sub>3</sub>, CC, AI, GOC, NGOC, OSI, and PCI.

(3) Four distinct HAWK pyrolysis heating rates (5, 10, 15, 25, and 50 °C/min) were used to analyze the entire rock samples for bulk kinetics modeling. The bulk kinetic model, which consists of a single frequency factor and an activation energy distribution, uses the produced bulk petroleum formation curves as input. Kinetics 2015 software is being used.

(4) Statistical treatment was carried out using the SPSS© program.

(5) The TOC, HI, and T<sub>max</sub> maps were drawn using the ArcMap 10.5 program.

## RESULTS AND DISCUSSION

### Statistical Treatment

The data obtained from the HAWK pyrolysis technique are listed in Tables 1 and 2. The statistical treatment included descriptive statistics (Table 3), correlation matrix (Table 4), principal component analysis (Table 5 and Fig. 4), and cluster analysis (Fig. 5 and Table 6).

**Table 1. HAWK pyrolysis data of the Hot Shale Member in wells B1-23 and Q1-23**

Well ID	Sample ID	Depth (ft)	TOC	S1	S2	S3	PP	OI	HI	T <sub>max</sub>
Q1-23	2942-9652	9652	1.05	0.38	2.38	0.12	2.76	11	225	441
	2951-9682	9682	3.87	3.14	22.4	0.6	25.5	15	578	439
	2954-9691	9691	1.71	0.74	4.84	0.37	5.58	21	283	440
	9692	9692	1.89	0.79	5.58	0.49	6.37	25	294	440
	2964-9724	9724.4	9.94	5.15	23.4	1.24	28.6	12	235	439
	9744	9744	11.07	2.64	23.9	1	26.5	9	215	437
	2976-9763	9763	4.4	1.23	9.23	0.81	10.5	18	209	437
	9764	9764	4.19	1.33	10	0.67	11.3	16	238	439
	2979-9773	9773.62	6.84	1.59	8.64	2.87	10.2	41	126	430
B1-23	1401-07	4595.28	2.16	0.43	6.88	0.6	7.31	27	317	432
	1410-16	4625	2.26	0.57	6.47	0.32	7.04	14	286	432
	1419-25	4654.32	3.48	0.93	12.9	0.35	13.8	10	369	431
	4674	4674	2.47	1.35	19.6	0.51	21	21	794	425
	1428-34	4683.84	11.91	3.05	59.1	0.95	62.1	8	495	428
	1434	4703.52	9.75	3.29	60.1	1.15	63.4	11	615	423
	1437-43	4713.36	12.39	4.13	73.5	1.99	77.7	16	593	421
	4733	4733	5.34	0.84	28.3	1.38	29.2	26	531	417

**Table 2. HAWK pyrolysis data of the Hot Shale Member in wells B1-23 and Q1-23**

Well ID	Ro	AI	CaCO <sub>3</sub>	CC	GOC	PI	NGOC	OSI	PCI
Q1-23	0.78	0.86	3	0.36	0.26	0.14	0.79	36.2	2.29
	0.74	3.17	39.8	4.77	2.21	0.12	1.66	81.1	21.2
	0.76	1.4	6.92	0.83	0.5	0.13	1.21	43.3	4.63
	0.76	1.55	19.8	2.38	0.57	0.12	1.32	41.8	5.29
	0.74	8.15	6.33	0.76	2.48	0.18	7.47	51.8	23.7
	0.71	9.08	7.68	0.92	2.3	0.1	8.77	23.9	22
	0.71	3.61	6.2	0.74	0.93	0.12	3.47	28	8.68
	0.74	3.43	10.78	1.29	1	0.12	3.18	31.7	9.41
	0.58	5.61	2.21	0.26	1	0.16	5.84	23.3	8.49
B1-23	0.62	1.77	3.06	0.37	0.65	0.06	1.51	19.9	6.07
	0.62	1.86	3.34	0.4	0.62	0.08	1.64	25.2	5.84
	0.6	2.86	8.39	1	1.19	0.07	2.29	26.7	11.5
	0.5	2.03				0.06		54.7	17.4
	0.54	9.77	12.6	1.51	5.33	0.05	6.58	25.6	51.6
	0.5	8	55.6	6.67	5.46	0.05	4.29	33.7	52.6
	0.42	10.2	70	8.4	6.71	0.05	5.69	33.3	64.5
	0.3	4.38				0.03		15.7	24.2

(AI = adsorption index; CaCO<sub>3</sub> = calcium carbonate equivalent (wt%); CC = carbonate carbon (wt%); GOC = generative organic carbon; HI = hydrogen index (mg/g); NGOC = non-generative organic carbon; OI = oxygen index (mg/g); OSI = oil saturation index; PCI = pyrolyzable carbon index (mg/g); PI = production index; PP = petroleum potential (mg/g); Ro = vitrinite reflectance (wt%); S1 = quantity of free hydrocarbons (mg/g); S2 = quantity of thermally generated (cracked) hydrocarbons (mg/g); S3 = quantity of CO<sub>2</sub> generated during pyrolysis (mg/g); T<sub>max</sub> = temperature at which maximum rate of generation of hydrocarbons occurs (°C); TOC = total organic carbon (wt%))

The descriptive statistics show that there is a large variation in the values of analyzed parameters. This large range indicates a variation in the organic richness, petroleum potential, and thermal maturity as well as the presence of different kerogen types. In the correlation matrix, S1 and S2 have positive correlations with TOC (r = 0.83 and 0.82, respectively), which indicates the influence of S1 and S2 from TOC. Moreover, the weak

negative correlation shown by  $T_{max}$  and  $Ro$  with TOC ( $r = -0.39$  and  $-0.37$ , respectively) suggests that thermal maturity is unaffected by the amount of organic matter.

**Table 3. Descriptive statistics of the analyzed parameters**

Parameters	N	Minimum	Maximum	Mean
TOC	17	1.05	12.4	5.57
S1	17	0.38	5.15	1.86
S2	17	2.38	73.5	22.2
S3	17	0.12	2.87	0.91
PP	17	2.76	77.7	24
OI	17	8	41	17.7
HI	17	126	794	377
$T_{max}$	17	417	441	432
$Ro$	17	0.3	0.78	0.62
AI	17	0.86	10.2	4.57
CaCO <sub>3</sub>	15	2.21	70	17.1
CC	15	0.26	8.4	2.04
GOC	15	0.26	6.71	2.08
PI	17	0.03	0.18	0.1
NGOC	15	0.79	8.77	3.71
OSI	17	15.7	81	34.5
PCI	17	2.29	64	20

**Table 4. Correlation matrix of the analyzed parameters**

	TOC	S1	S2	S3	OI	HI	$T_{max}$	$Ro$	AI	CaCO <sub>3</sub>
TOC	1.00									
S1	0.83	1.00								
S2	0.82	0.71	1.00							
S3	0.61	0.44	0.42	1.00						
OI	-0.30	-0.37	-0.35	0.50	1.00					
HI	0.17	0.27	0.61	-0.04	-0.18	1.00				
$T_{max}$	-0.39	-0.14	-0.64	-0.46	-0.15	-0.65	1.00			
$Ro$	-0.37	-0.11	-0.61	-0.47	-0.19	-0.63	0.99	1.00		
AI	1.00	0.83	0.82	0.61	-0.31	0.17	-0.39	-0.37	1.00	
CaCO <sub>3</sub>	0.37	0.35	0.69	0.33	-0.01	0.84	-0.72	-0.72	0.37	1.00

The principal component analysis yielded three components. A simplified explanation of these components is given below:

**First principal component (PC1):** It is the most potent component, making up roughly 59.61% of the variables. Positive loading is seen for TOC, S1, S2, PP, HI, AI, CaCO<sub>3</sub>, CC, GOC, and PCI in this component. Furthermore, it loads negatively for  $T_{max}$  and  $Ro$ . This component appears to be important for interpreting the organic richness, petroleum potential, thermal maturity and kerogen type.

**Second principal component (PC2):** 15.62% of all variables are accounted for by this component. Positive loading is evident for S3 and NGOC. HI exhibits negative loading. It seems that this component is also essential to comprehending the kerogen type.

**Third principal component (PC3):** This component clarifies 12.8% of all variables. For OSI, negative loading is obvious. This component is essentially irrelevant.

The dendrogram cluster analysis divided the TOC content into three different groups, while the division of the rest of the source rock properties is unclear. Below is a description of the three TOC groups:

**Group I:** The samples of this group have the lowest TOC content (1.05-2.47%).

**Group II:** Compared to Group I, this group contains more TOC content (3.48-6.84%).

**Group III:** The highest TOC content (9.75-12.39%) is found in this group.

**Table 5. Principal component analysis of the analyzed parameters**

<b>Eigenvalues</b>	10.13	2.65	2.18
<b>% of Variance</b>	59.61	15.62	12.80
<b>Cumulative %</b>	59.61	75.22	88.03

Principal components	PC1	PC2	PC3
TOC	0.87	0.44	0.15
S1	0.77	0.24	0.55
S2	0.99	-0.07	0.01
S3	0.50	0.66	-0.12
PP	0.99	-0.05	0.05
OI	-0.32	0.34	-0.34
HI	0.75	-0.62	0.06
T <sub>max</sub>	-0.80	0.01	0.55
Ro	-0.80	-0.02	0.56
AI	0.87	0.44	0.15
CaCO <sub>3</sub>	0.79	-0.43	0.11
CC	0.79	-0.43	0.11
GOC	0.99	-0.04	0.04
PI	-0.56	0.45	0.58
NGOC	0.59	0.74	0.20
OSI	-0.01	-0.40	0.82
PCI	0.99	-0.05	0.05

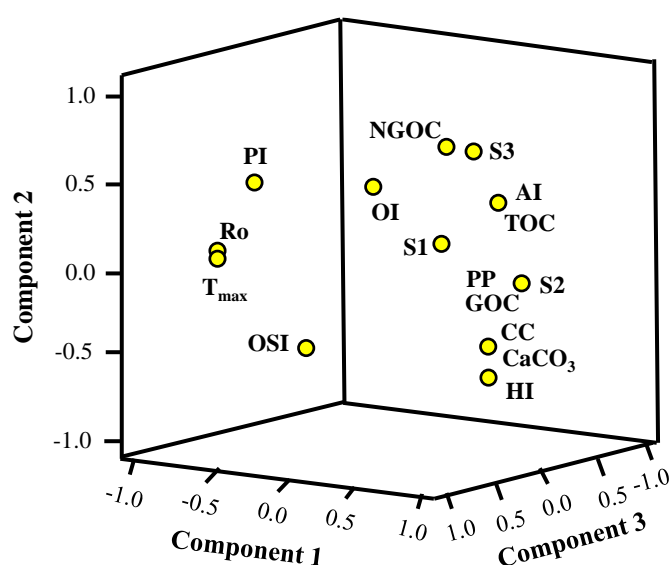


**Figure 4.** Plot of PC loadings of the analyzed parameters.

### Organic Richness

Petroleum should be produced in proportion to the amount of organic richness in the source rock since it is a byproduct of the organic matter that are distributed in the source rock [22]. The TOC content of sedimentary rocks is a crucial criterion for assessing their organic richness because it is a prerequisite for the production of oil or gas [23]. Peters and Cassa [24] categorized the organic richness into five classes based on the TOC content: (1) Poor (TOC ranges from 0 to 0.5%); (2) Fair (TOC ranges from 0.5 to 1%); (3) Good (TOC ranges from 1 to 2%); (4) Very good (TOC ranges from 2 to 4%); and (5) Excellent (TOC > 4%). The TOC values (1.05-12.39%) indicate that the organic richness of the Hot Shale Member ranges from good to excellent. This hypothesis is confirmed by the binary plot of TOC versus PP (Fig. 6). The TOC map is shown in Fig. 7.

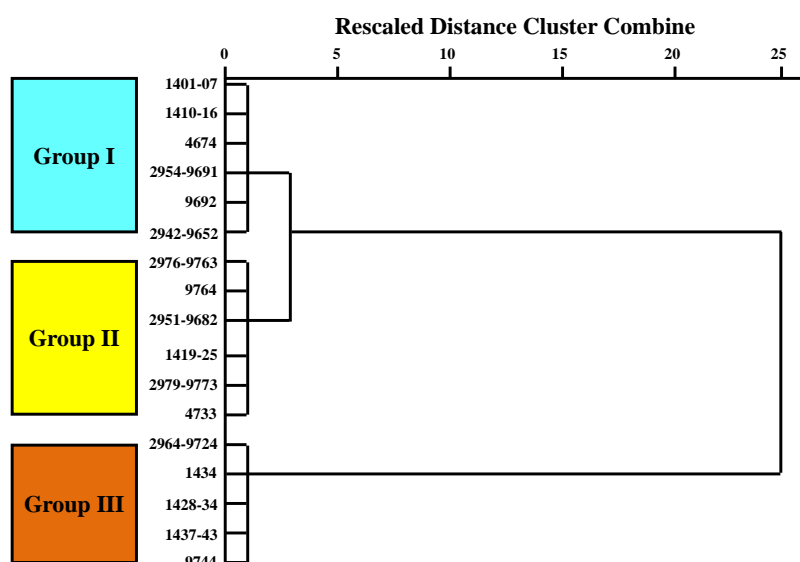


**Figure 5. Dendrogram from cluster analysis (Ward method) of the analyzed parameters.**

**Table 6. Cluster analysis of the analyzed parameters**

Parameters	Group I	Group II	Group III
<b>TOC</b>	1.05-2.47	3.48-6.84	9.75-12.4
<b>S1</b>	0.38-1.35	0.84-3.14	2.64-5.15
<b>S2</b>	2.38-19.6	8.64-28.3	23.4-73.5
<b>S3</b>	0.12-0.6	0.35-2.87	0.95-1.99
<b>PP</b>	2.76-21	10.2-29.1	26.5-77.7
<b>OI</b>	11-27	10-41	8-16
<b>HI</b>	225-794	126-578	215-615
<b>T<sub>max</sub></b>	425-441	417-439	421-439
<b>Ro</b>	0.5-0.78	0.3-0.74	0.42-0.74
<b>AI</b>	0.86-2.03	2.86-5.61	8-10.2
<b>CaCO<sub>3</sub></b>	3-19.8	2.21-39.8	6.33-70
<b>CC</b>	0.36-2.38	0.26-4.77	0.76-8.4
<b>GOC</b>	0.26-0.65	0.93-2.21	2.3-6.71
<b>PI</b>	0.06-0.14	0.03-0.16	0.05-0.18
<b>NGOC</b>	0.79-1.64	1.66-5.84	4.29-8.77
<b>OSI</b>	19.9-54.7	15.7-81.1	23.9-51.8
<b>PCI</b>	2.29-17.4	8.49-24.2	22-64.5

### Kerogen Type

The portion of organic matter found in sedimentary rocks known as kerogen is insoluble in typical organic solvents. Kerogens are composed of various organic matter [22]. Based on the HI values, Peters and Cassa [24] classified kerogen into five classes: (1) Type I (HI>600 mg/g); (2) Type II (HI ranges from 300 to 600 mg/g); (3) Type II-III (HI ranges from 200 to 300 mg/g); (4) Type III (HI ranges from 50 to 200 mg/g); and (5) Type IV (HI<50 mg/g). In the Hot Shale Member, the presence of various kerogen types, including types I, II, and III, is indicated by the HI values (126-794 mg/g). The binary plots of OI versus HI (Fig. 8), TOC versus S2 (Fig. 9), and T<sub>max</sub> versus HI (Fig. 10) provide additional evidence for this assumption. Fig. 11 shows the HI map.

### Indigeneity

Hydrocarbons in source rocks are classified into: (1) Indigenous hydrocarbons; and (2) Nonindigenous hydrocarbons. The S1/TOC ratio has been used to determine the type of hydrocarbons. Values below 1.5 are thought to represent indigenous hydrocarbons, while values above 1.5 are indicative of nonindigenous hydrocarbons [25]. In the Hot Shale Member, the S1/TOC ratio ranges from 0.16 to 0.81, indicating the dominance of indigenous hydrocarbons. The binary plot of TOC versus S1 (Fig. 12) supports this hypothesis.

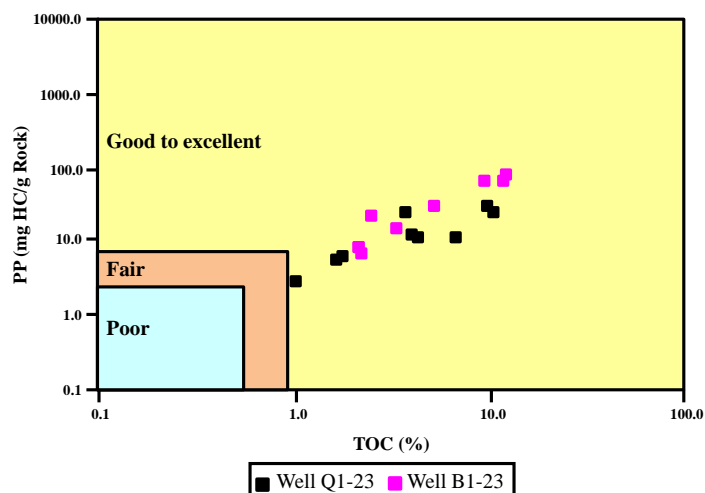


**Figure 6. Binary plot of TOC vs. PP showing the organic richness of the Hot Shale Member (fields after [22]).**

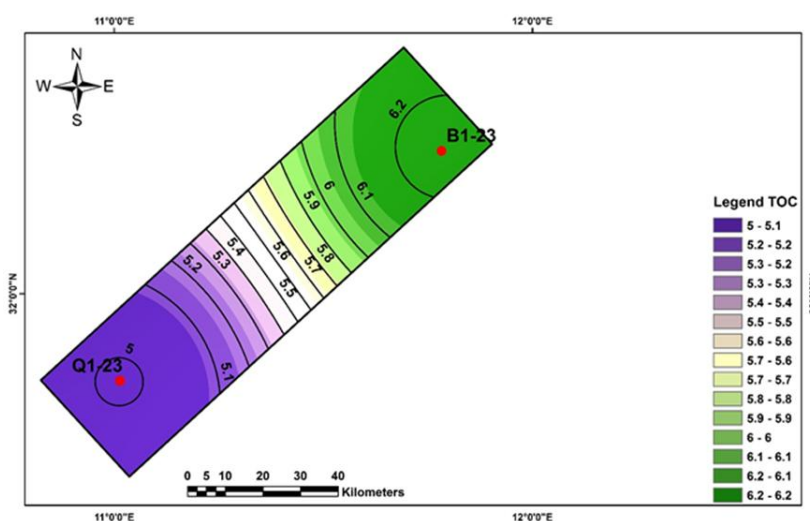


**Figure 7. TOC map between the studied wells.**

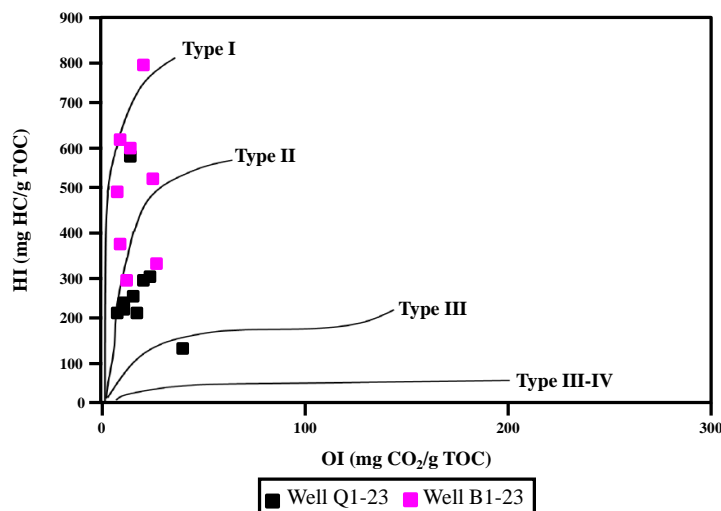


**Figure 8. Binary plot of OI vs. HI showing the kerogen type for the Hot Shale Member (fields after [26]).**



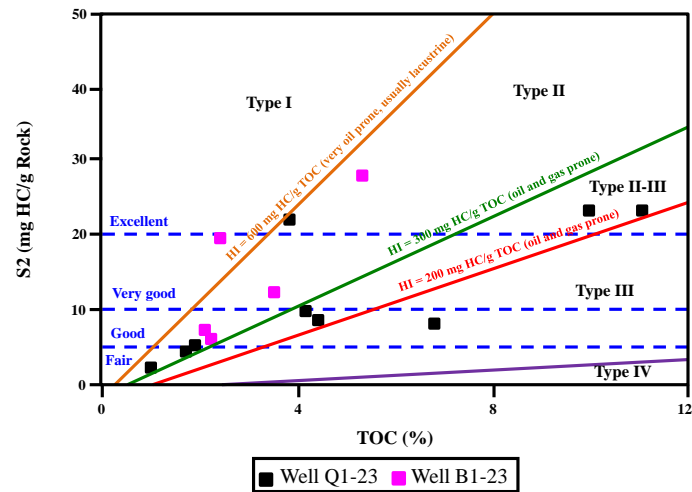


Figure 9. Binary plot of TOC vs. S2 showing the kerogen type for the Hot Shale Member (fields after [27]).

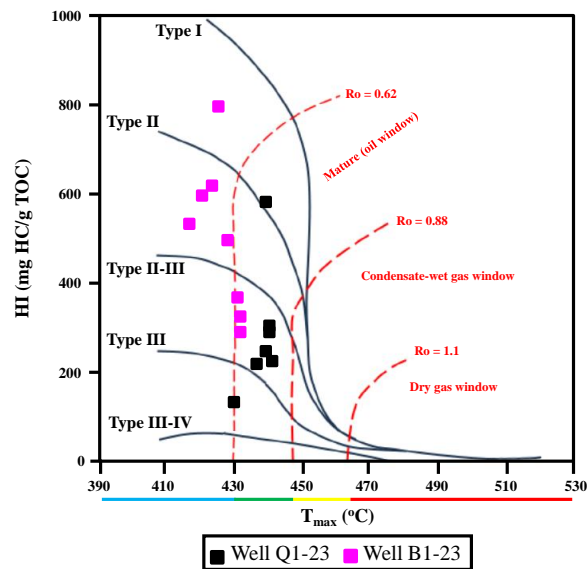


Figure 10. Binary plot of  $T_{max}$  vs. HI showing the kerogen type and thermal maturity for the Hot Shale Member (fields after [28]).

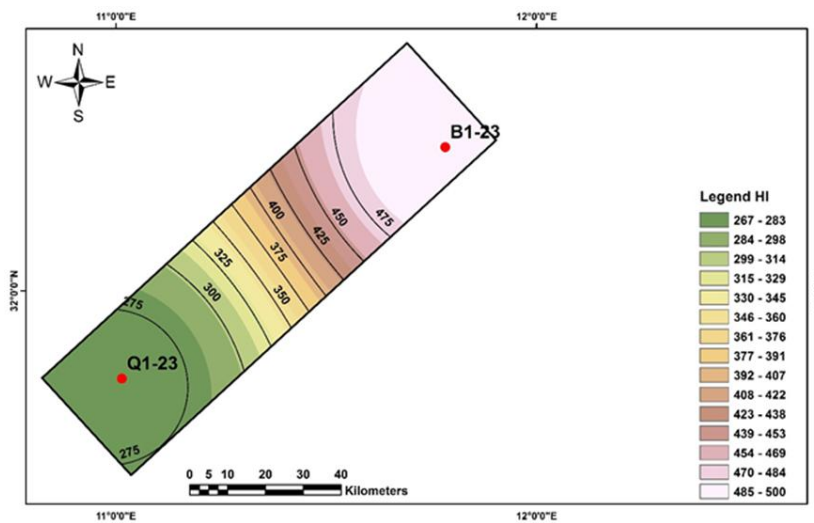
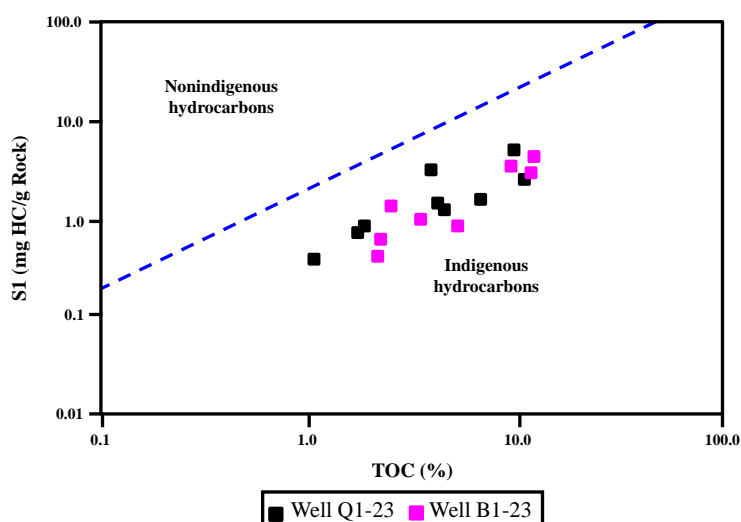


Figure 11. HI map between the studied wells.



**Figure 12. Binary plot of TOC vs. S1 showing the hydrocarbon type in the Hot Shale Member (fields after [25]).**

### Thermal Maturity

Thermal maturity refers to how much the chemical composition of organic matter is altered by heat reactions. Source rock maturation, reservoir diagenesis, and porosity development are all influenced by thermal maturity and burial history [29]. Numerous parameters, such as  $T_{max}$  and  $R_o$  can be used to assess the degree of thermal maturity of organic matter [24]. Based on the values of  $T_{max}$  and  $R_o$ , Peters and Cassa [24] identified six grades of maturity (Table 7). The binary plots of  $T_{max}$  versus HI (Fig. 10),  $T_{max}$  versus  $R_o$  (Fig. 13), and PI versus  $T_{max}$  (Fig. 14) indicate that most of the samples of well B1-23 contain immature organic matter, while mature organic matter predominate in the samples of well Q1-23. The values of  $T_{max}$  (417-441 °C) and  $R_o$  (0.3-0.78%) support the aforementioned assumption. Fig. 15 presents the  $T_{max}$  map.

**Table 7. Geochemical parameters characterizing the degree of thermal maturity (after [24])**

Degree of thermal maturity	$R_o$ (%)	$T_{max}$ (°C)
Immature	0.2-0.6	<435
Early mature	0.6-0.65	435-445
Peak mature	0.65-0.9	445-450
Late mature	0.9-1.35	450-470
Postmature	>1.35	>470

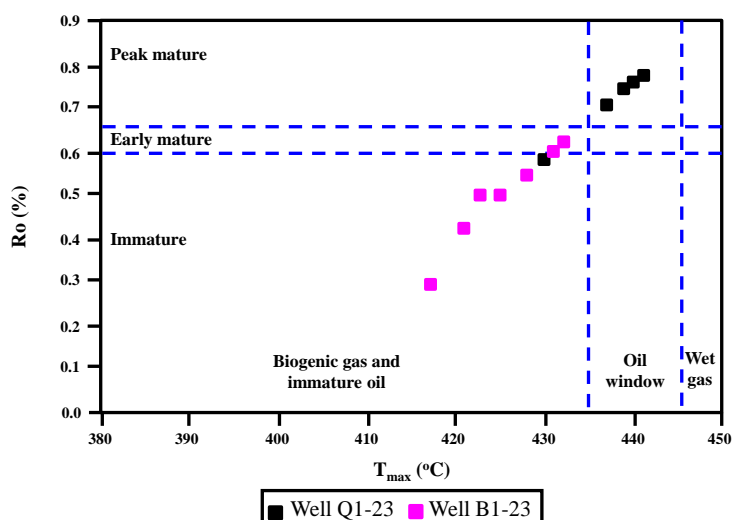


**Figure 13. Binary plot of  $T_{max}$  vs.  $R_o$  showing the thermal maturity for the Hot Shale Member (fields after [30]).**

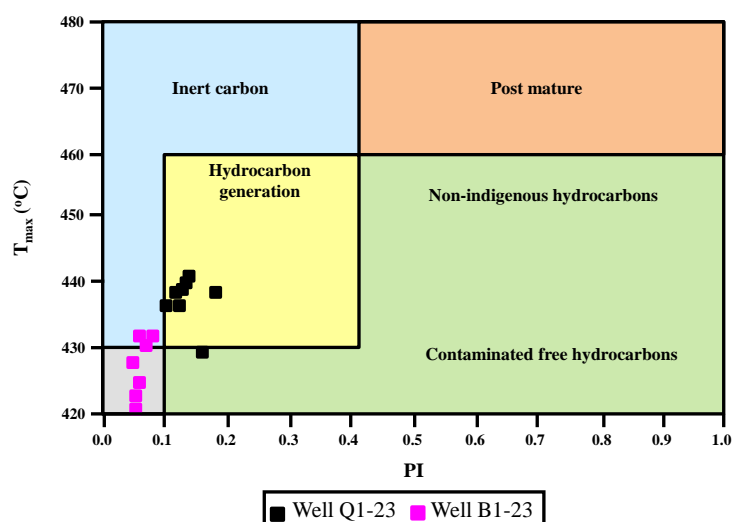


**Figure 14. Binary plot of PI vs.  $T_{max}$  showing the thermal maturity for the Hot Shale Member (fields after [31]).**

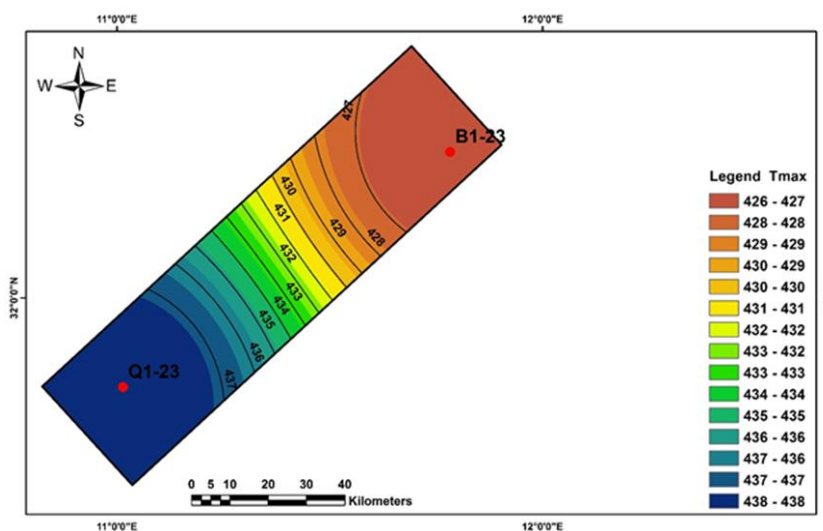


**Figure 15.  $T_{max}$  map between the studied wells.**

### Petroleum Potential

As mentioned previously in this work, the Hot Shale Member contains different types of kerogen in addition to variations in TOC content and levels of thermal maturity. These findings suggest that the Hot Shale Member has a range of petroleum potential. The binary plot of TOC versus HI (Fig. 16) provides additional support for this hypothesis.

### Kinetic Parameters

Kerogen reactivity, which regulates the depth and temperature of oil and gas generation windows as well as the onset and rate of hydrocarbon generation, is reflected in source rock kinetics. Consequently, knowing source rock kinetics is essential for determining production sweet spots as well as quantitative resource modeling [33]. Tables 8 and 9 display the kinetics parameters of the Hot Shale Member. The activation energies (47-84 kcal/mol) are gaussian in shape (Figs. 17 and 18).

### CONCLUSION

A geochemical assessment was done of the Hot Shale Member of the Tanezzuft Formation (Early Silurian) in wells B1-23 and Q1-23, Ghadames Basin, NW Libya. The following are the work's conclusions:

- (1) The organic richness of the Hot Shale Member ranges from good to excellent.
- (2) The Hot Shale Member holds kerogens of types I, II, and III.
- (3) The Hot Shale Member contains indigenous hydrocarbons.
- (4) Mature organic matter predominate in well Q1-23 samples, while immature organic matter are present in the majority of well B1-23 samples.
- (5) There is a range of petroleum potential in the Hot Shale Member.
- (6) The activation energies are gaussian-shaped.

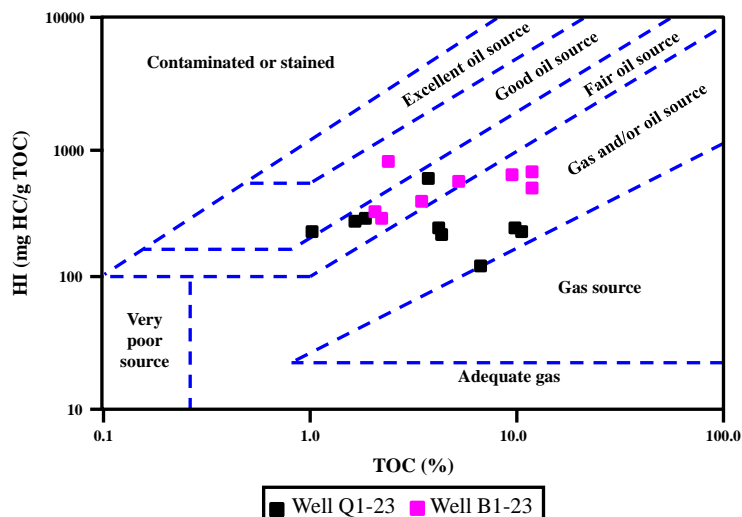


**Figure 16. Binary plot of TOC vs. HI showing the petroleum potential for the Hot Shale Member (fields after [32]).**

**Table 8. Kinetics parameters of the Hot Shale Member in well Q1-23**

Percent	Activation energy (cal/mol)
1.15	84000
1.63	49000
1.42	50000
0.00	51000
2.14	52000
49.15	53000
8.37	54000
25.74	55000
0.00	56000
0.00	57000
10.40	58000
Frequency factor = 1000E+14 s <sup>-2</sup>	

**Table 9. Kinetics parameters of the Hot Shale Member in well B1-23**

Percent	Activation energy (cal/mol)
1.03	47000
0.87	48000
1.02	49000
0.00	50000
10.25	51000
47.06	52000
14.27	53000
14.64	54000
4.70	55000
1.96	56000
4.19	57000
Frequency factor = 1000E+14 s <sup>-2</sup>	

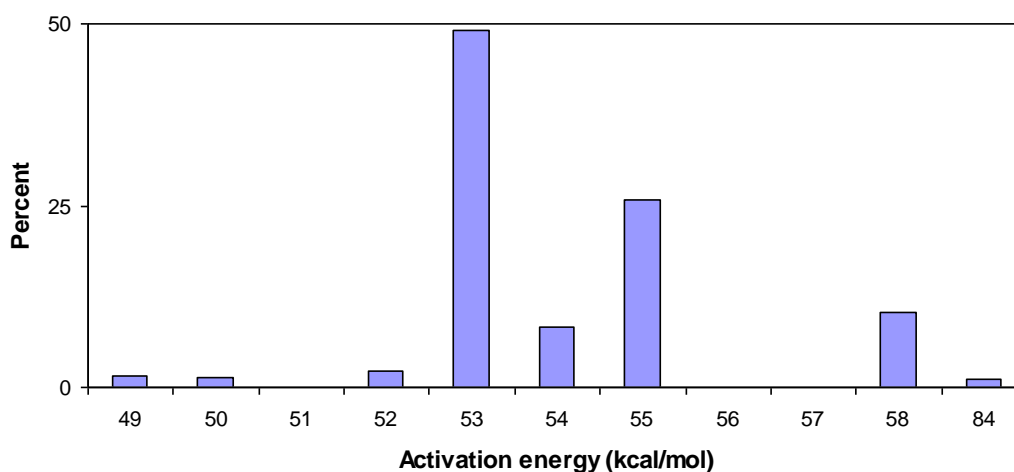


**Figure 17. Activation energies of the Hot Shale Member in well Q1-23.**

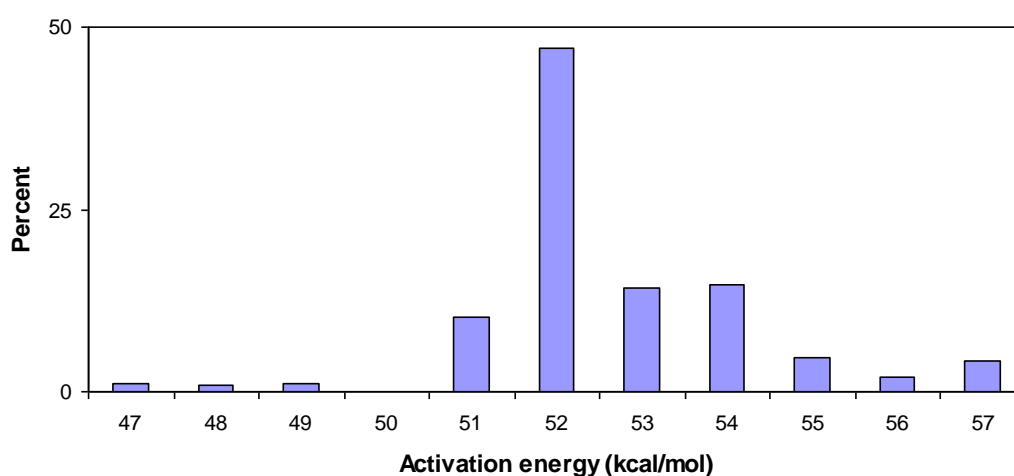


**Figure 18. Activation energies of the Hot Shale Member in well B1-23.**

### Recommendation

Large reserves of unconventional hydrocarbons, such as shale gas and shale oil, are found in Libya. The Hot Shale Member is considered one of the unconventional reservoirs in Libya. The formation of shale oil and shale gas depends on several factors, including high TOC content and high thermal maturity. The current study showed that both of the previous factors are available in the Hot Shale Member in wells B1-23 and Q1-23. Therefore, the authors recommend conducting an analysis of biomarkers to evaluate unconventional hydrocarbons in the studied wells.

### Acknowledgments

The authors are grateful to Sirte Oil Company, Libya, for providing the data. Special thanks to the geochemical laboratory that prepared and analyzed the samples.

### Conflicts of Interest

Declare conflicts of interest or state "The authors declare no conflicts of interest." Authors must identify and declare any personal circumstances or interest that may be perceived as inappropriately influencing the representation or interpretation of reported research results.

### References

- Desio A. Prime notizie sulla presenza del Silurico fossilifero nel Fezzan. Bollettino della Società geologica italiana. 1936;55:116-120.
- Klitzsch E. Ein profil aus dem typusgebiet gotlandischer und devonische schichten der zentralsahara (westrand Murzukbecken, Libyen). Erdol und Kohle Deut. 1965;18:605-607.
- Shalbak FA. Palaeozoic petroleum systems of the Murzuq Basin, Libya. Unpublished PhD Thesis, Barcelona University, Spain. 2015.

4. El Diasty WS, El Beialy SY, Fadeel FI, Batten DJ. Palynostratigraphic, palynofacies, organic geochemical and palaeoenvironmental analysis of the Silurian Tanezzuft Formation in the Ghadames Basin of north-west Libya. *Revue de Micropaléontologie*. 2019;62(1):45-58.
5. de Castro JC, Della Favera JC, El-Jadi M. Tempestite facies, Murzuq Basin, Great Socialist People's Libyan Arab Jamahiriya: their recognition and stratigraphic implications. In: M.J. Salem and M.N. Belaid (eds) 3th Symposium on the Geology of Libya. Elsevier, Amsterdam. 1991;5:1757-1760.
6. Hallett D, Clark-Lowes D. Petroleum geology of Libya. 2nd edition, Amsterdam, Elsevier Inc., 2016:404p.
7. Lüning S, Adamson K, Craig J. Frasnian 'Hot Shales' in North Africa: Regional Distribution and Depositional Model. In: Arthur, T. J., Macgregor, D. S., Cameron, N. (Eds.), *Petroleum Geology of Africa: New Themes and developing technologies*. Geological Society, London, Special Publication. 2003;207:165-184.
8. Hallett D. *Petroleum geology of Libya*. Amsterdam, Elsevier Inc., 2002:503p.
9. Hrouda M. The hydrocarbon source potential of the Palaeozoic rocks of the Ghadames Basin, NW Libya. Unpublished PhD Thesis, University of Newcastle, UK. 2004.
10. Fello N, Lüning S, Storch P, Redfern J. Identification of early Llandovery (Silurian) anoxic palaeo-depressions at the western margin of the Murzuq Basin (southwest Libya), based on gamma-ray spectrometry in surface exposures. *GeoArabia*. 2006;11(3):101-118.
11. EIA (U.S. Energy Information Administration). Technically recoverable shale oil and shale gas resources: Libya. Technical Report. 2015:26p.
12. Meinhold G, Le Heron DP, Elgady M, Abutarruma Y. The search for 'hot shales' in the western Kufra Basin, Libya: Geochemical and mineralogical characterisation of outcrops, and insights into latest Ordovician climate. *Arabian Journal of Geosciences*. 2016;9(62).
13. El Diasty WS, El Beialy SY, Anwari TA, Peters KE, Batten DJ. Organic geochemistry of the Silurian Tanezzuft Formation and crude oils, NC115 concession, Murzuq Basin, southwest Libya. *Marine and Petroleum Geology*. 2017;86:367-385.
14. Aboghlila S, Elaalem M, Ezlit Y, Farifr E. Geochemical characteristics of six formations based on organic geochemical parameters, Murzuq Basin, Libya. *Advances in Research*. 2018;15(4):1-11.
15. Musa MO. Thermal maturity and time of oil generation of the source rock, Murzuq Basin. *Albayan Scientific Journal*. 2019;4:194-206.
16. Albaghdady A, Aboghlila S, Farifr E, Ramadan M, Alburki A. Source Rock Characterization of Silurian Tanezzuft and Devonian Awaynat Wanin formations the northern edge of the Murzuq Basin, south west Libya. *Petroleum and Petrochemical Engineering Journal*. 2020;4(1):000216.
17. Shaltami OR, Bustany I, Fares FF, Errishi H, EL Oshebi FM. Unconventional hydrocarbons in the Hot Shale Member of the Tanezzuft Formation. 1st edition, Amazon Kindle Direct Publishing (KDP). 2021:123p.
18. Albriki K, Wang F, Li M, El Zaroug R, Ali A, Samba M, Wiping F, Mohammed RS. Silurian hot shale occurrence and distribution, organofacies, thermal maturation, and petroleum generation in Ghadames Basin, North Africa. *Journal of African Earth Sciences*. 2022;189:104497.
19. Carr ID. Second-order sequence stratigraphy of the Palaeozoic of North Africa. *Journal of Petroleum Geology*. 2002;25:259-280.
20. Haq BU, Schutter SR. A chronology of Palaeozoic sea-level changes. *Science*. 2008;322:64-68.
21. Galeazzi S, Point O, Haddadi N, Mather J, Druesne D. Regional geology and petroleum systems of the Illizi-Berkine area of the Algerian Saharan Platform: An overview. *Marine and Petroleum Geology*. 2010;27:143-178.
22. Tissot BP, Welte DH. *Petroleum formation and occurrence*. 2nd edition. Springer Berlin, Heidelberg. 1984:702p.
23. Hsu CS, Robinson PR. *Practical advances in petroleum processing*. 1st edition, Springer New York. 2006:866p.
24. Peters KE, Cassa MR. Applied source rock geochemistry. In: Magoon, L.B., Dow, W.G. (Eds.): *The petroleum system from source to trap*, AAPG Memoir. 1994;60:93-117.
25. Van Krevelen DW. *Coal: typology-chemistry-physics-constitution*. Elsevier Science, Amsterdam. 1961:514p.
26. Longford FF, Blanc-Valleron MM. Interpreting Rock-Eval pyrolysis data using graphs of pyrolyzable hydrocarbons vs. total organic carbon. *American Association of Petroleum Geologists (AAPG) Bulletin*. 1990;74:799-804.
27. Hall LS, Boreham CJ, Edwards DS, Palu TJ, Buckler T, Hill AJ, Troup A. Cooper Basin source rock geochemistry: Regional hydrocarbon prospectivity of the Cooper Basin. *Geoscience Australia*. 2016: Part2:62p.
28. Hunt JM. *Petroleum geochemistry and geology*. 2nd edition, W. H. Freeman. 1996:743p.
29. Pradier B, Bertrand P, Martinez L, Laggoun-Defarge F. Fluorescence of organic matter and thermal maturity assessment. *Organic Geochemistry*. 1991;17(4):511-524.
30. Atta-Peters D, Garrey P. Source rock evaluation and hydrocarbon potential in the Tano basin, South Western Ghana, West Africa. *International Journal of Oil, Gas and Coal Engineering*. 2014;2(5):66-77.
31. Hakimi MH, Abdullah WH, Shalaby MR. Source rock characterization and oil generating potential of the Jurassic Madbi Formation, onshore East Shabawah oilfields, Republic of Yemen. *Organic Geochemistry*. 2010;41(5):513-521.
32. Jackson KS, Hawkins PJ, Bennett AJR. Regional facies and geochemical evaluation of southern Denison Trough. *Journal of Australian Petroleum Production and Exploration*. 1985;20:143-158.
33. Cedeño A, Ohm S, Escalona A, Marin D, Olausson S, Demchuk T. Upper Jurassic to Lower Cretaceous source rocks in the Norwegian Barents Sea, part II: Insights from open- and closed-system pyrolysis experiments. *Marine and Petroleum Geology*. 2021;134:105343.

**المستخلص**

العمل الحالي هو تقييم للسخور المصدرية لعضو الصخر الزيتي الساخن في تكوين تنزفوت (السيلوري المبكر) باستخدام البيانات التي تم الحصول عليها من الآبار B1-23 و Q1-23 ، حوض غدامس، شمال غرب ليبيا. البيانات الجيوكيميائية التي تم الحصول عليها من تحليل أداة HAWK التي أجرتها شركة سرت للنفط على عدد من عينات الصخر الزيتي التي تمثل عضو الصخر الزيتي الساخن. من حيث الثراء العضوي، يقع عضو الصخر الزيتي الساخن بين الجيد والممتاز بناءً على قيم TOC (1.05-12.39%) يدعم الرسم البياني الثنائي لـ TOC مقابل PP هذا الافتراض. من حيث نوع الكيروجين، تُظهر قيم HI (126-794 مجم / جم) وجود أنواع مختلفة من الكيروجين، مثل الأنواع I و II و III. تقدم المخططات الثنائية لـ Tmax مقابل HI ، و TOC مقابل S2 ، و OI مقابل HI المزيد من الأدلة على هذه الفرضية. من حيث الأصالة، تشير نسبة S1/TOC (0.16-0.81) إلى هيمنة الهيدروكربونات الأصلية. ويعطي الرسم البياني الثنائي لـ TOC مقابل S1 مصداقية لهذا الافتراض. ومن حيث النضج الحراري، تشير قيم Tmax (417-441 درجة مئوية) و Ro (0.3-0.78%)، والرسم البياني الثنائي لـ Tmax مقابل HI ، و Tmax مقابل Ro ، و PI مقابل Tmax إلى أن عينات البئر Q1-23 تحتوي في المقام الأول على مادة عضوية ناضجة، في حين تحتوي غالبية عينات البئر B1-23 على مادة عضوية غير ناضجة. ومن حيث إمكانات البترول، يُظهر عضو الصخر الزيتي الساخن مجموعة متنوعة من إمكانات البترول، كما هو موضح في الرسم البياني الثنائي لـ TOC مقابل HI. ومن حيث المعلمات الحركية، فإن طاقات التنشيط (47-84 كيلو كالوري/مول) لها شكل غاوسي.